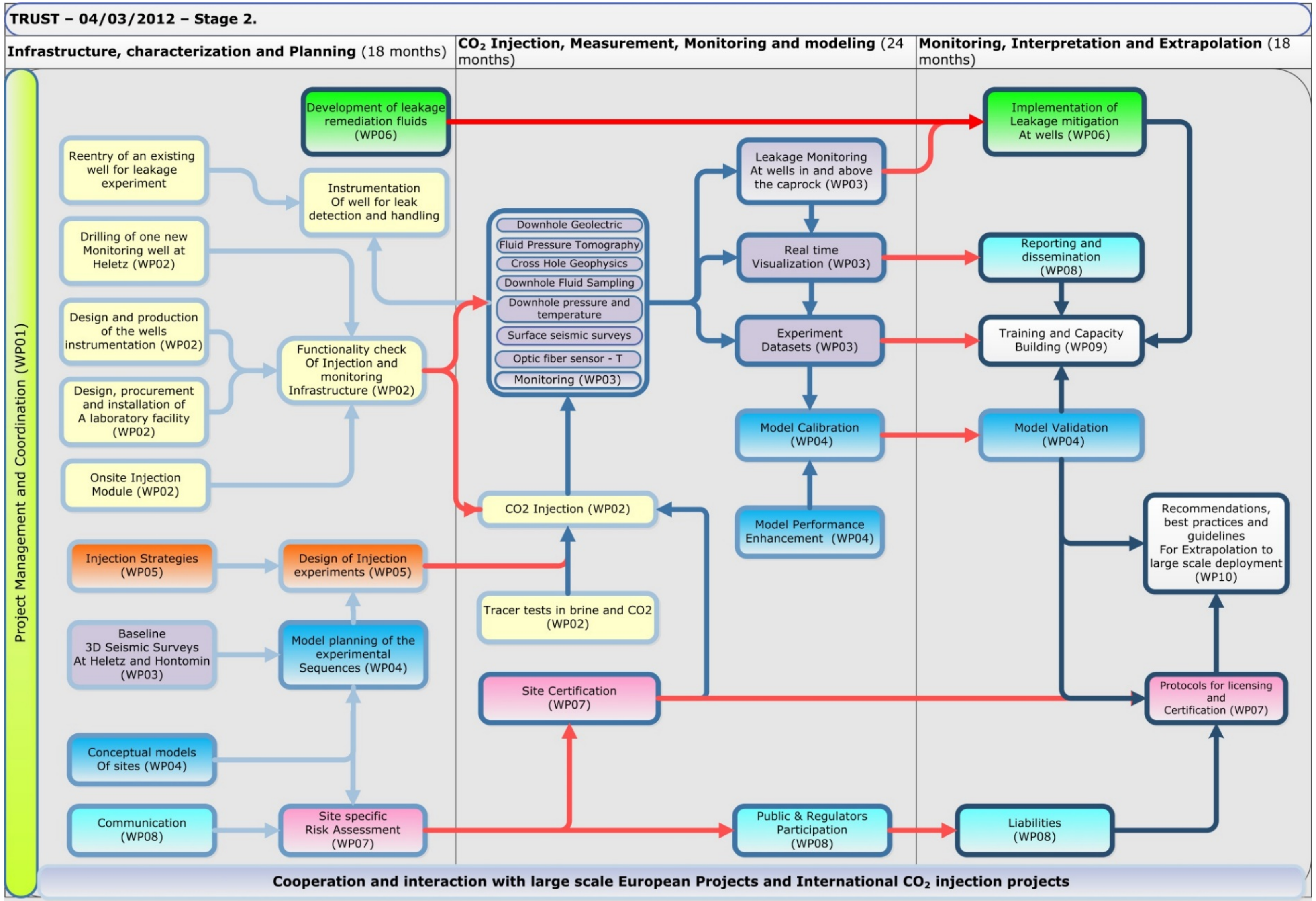

Workflow diagram of TRUST

The CO_2 heat exchanger

Pump skid during commissioning.

Utube sample lifting control panel.

Connection to the injection well

Transfer line for the measurement of the partial pressure of the CO_2 and the pH of the water in the high pressure sample.

Location of the shallow seismic wells, the injection well (H18A) and the monitoring well (H18B).

Selected snapshots during the CO_2 injection experiment at Heletz.


Snapshots during the repair of the injection well at Heletz.

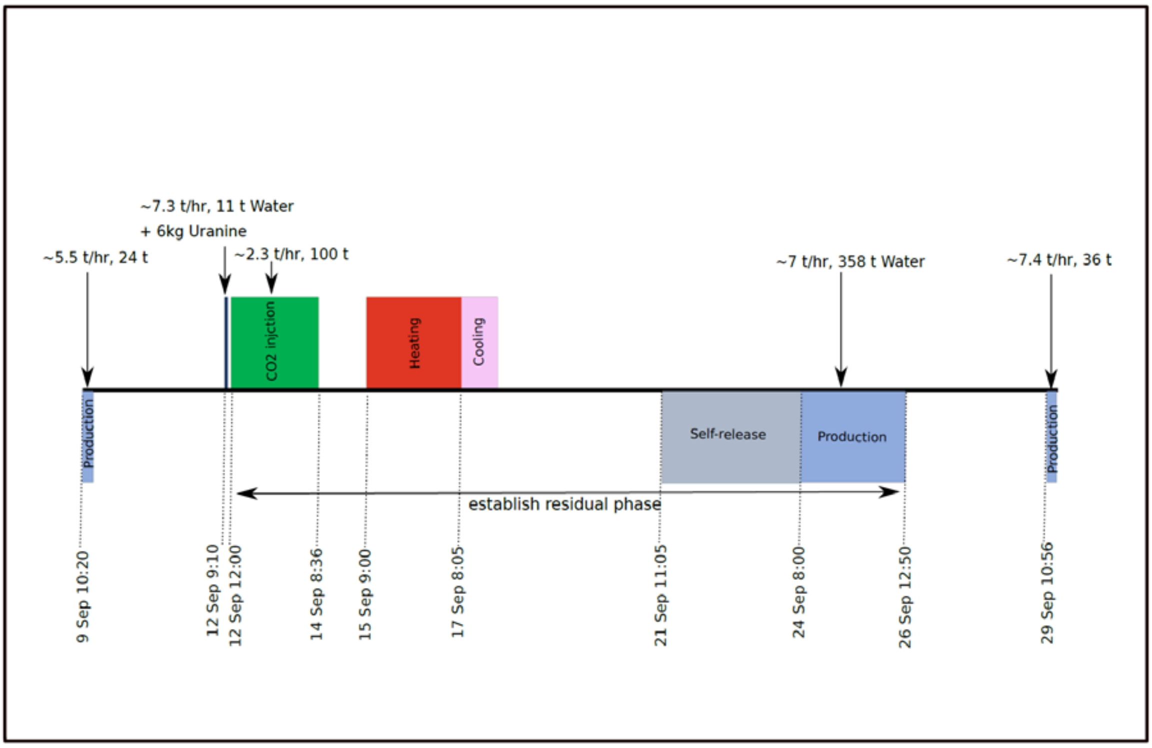

The overall test sequence of the Residual Trapping Experiment I (RTE I).

Key parameters of the different parts of the RTE I

Part of test sequence	Start time (date and time)	End time (date and time)	Total volume of fluid injected / pumped (Tons)	Average rate of injection / pumping (Tons / hour)	Main Monitoring / Sampling (*
Hydraulic reference test					
- Pumping	09-09-2016 10:20	09-09-2016 15:30	24	5.5	P,T, Q, Q_{tot}
- Recovery	09-09-2016 15:30	12-09-2016 9:10			P,T
Indicator tracer and water injection					
- Tracer injection	12-09-2016 9:19	12-09-2016 9:50	0.0058		P,T, Q, Q_{tot} Q_{tr}, Q_{tot-tr}
- Water injection	12-09-2016 9:10	12-09-2016 10:37	11	7.1	P,T,Q, Q_{tot}
CO_2 injection	12-09-2016 12:00	14-09-2016 8:36	100	2.3	P,T, Q_{co2}, $Q_{co2-tot}$
Heating experiment					
- Heating	15-09-2016 9:00	17-09-2016 8:05			P,T
- Cooling					
Establishing the residually trapped zone					
- Self Release	21-09-2016 11:05	24-09-2016 8:00			P,T, Q, Q_{tot}
- Active pumping of fluids	24-09-2016 8:00	26-09-2016 12:50	358	5-7	P,T, Q, Q_{tot}, S, TiT
Hydraulic test with residually trapped CO_2					
- Pumping	29-09-2016 10:56	29-09-2016 15:26	36	7.4	P,T, Q, Q_{tot}
- Recovery	29-09-2016 15:26	30-09-2016 01:33			P,T

P/T: downhole pressure and temperature – continuous measurement throughout the experiment
DTS: distributed temperature sensor - continuous measurement throughout the experiment
TiT: high pressure fluid sampling with Tube-in-tube (U-tube)
S: low pressure water and tracer sampling
Q: flow rate (water or CO_2)
Q_{tot}: total cumulative flow
Q_{tr}: rate of tracer injection
Q_{tr-tot}: total cumulative volume of tracer injected

Selected snapshots during the repair of the injection well at Heletz. The upper right picture shows one of the many holes that were found along the TiT.

Digital borehole receivers together with the seismic array controller.

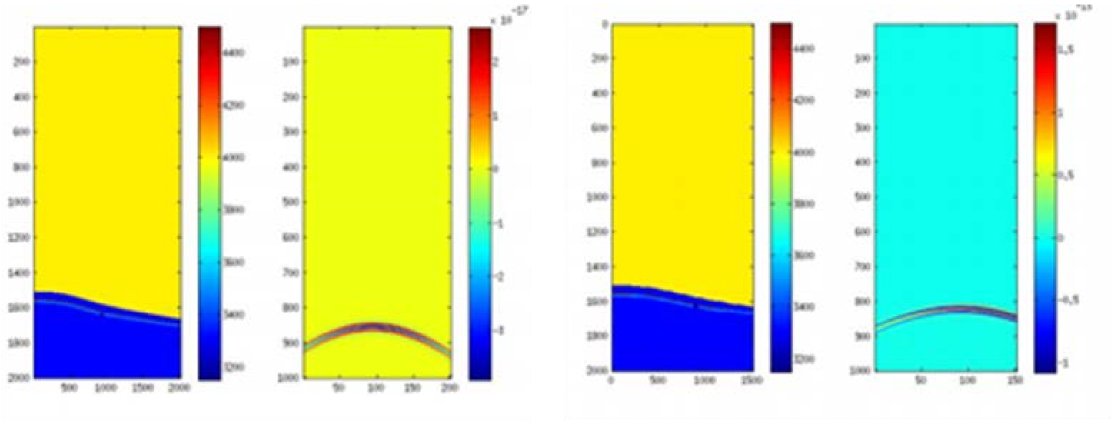

Velocity slices from repeat line models and shot gather differences between baseline and repeat line, 2D data sets (left) 3D data sets (right).

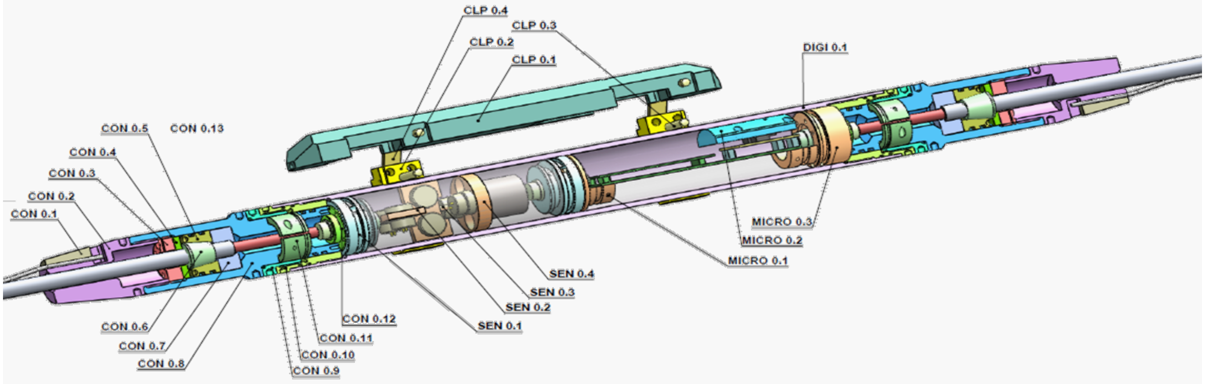

Down-hole receiver developed by Vibrometric includes: 3 orthogonal components - double 14 Hz geophones - and a 4th component, which is a low frequency (2 Hz) vertical geophone.

Layout of instrumentation deployment for near surface seismic monitoring at Heletz. Well A (orange) is in the North, Well B (yellow) is in the West and Well C (green) is in the South.

Installation of the buried receivers for the sub-surface monitoring array.

VIBSIST-3000 seismic source in the fields at Heletz in December 2017.

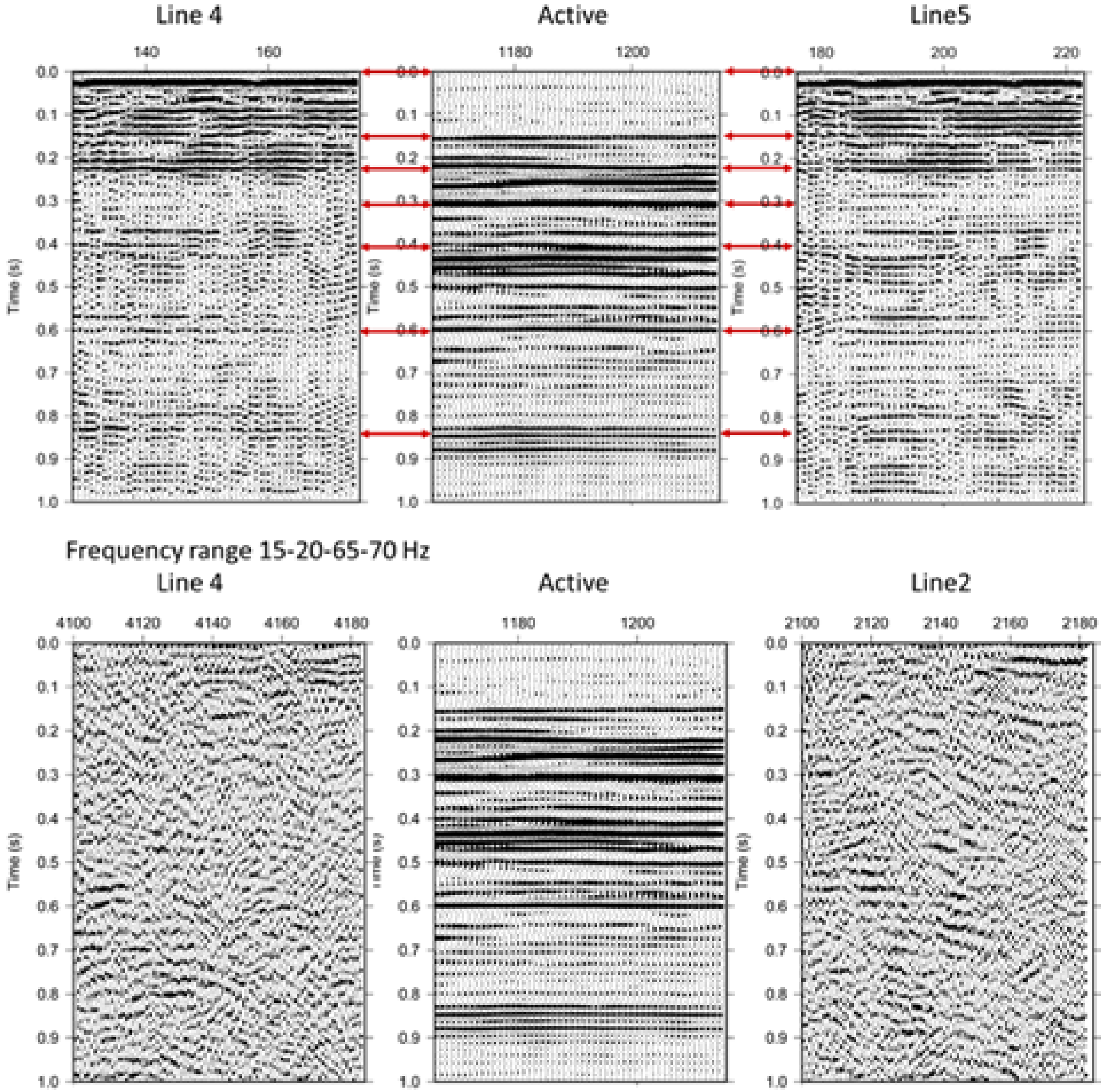

An example comparison of autocorrelation and cross-correlation processing results with stacked sections of active data sets.

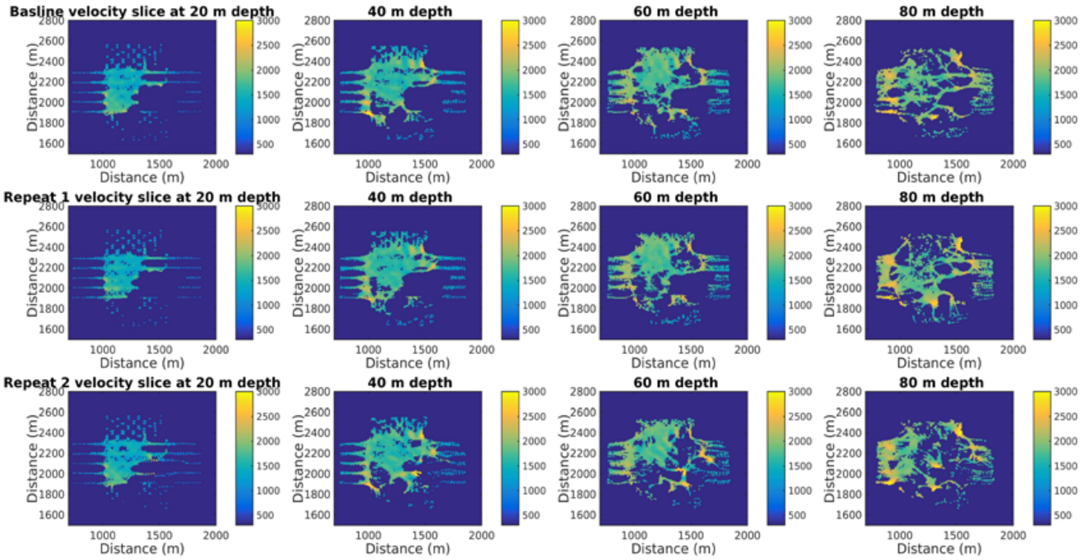

3D travel time tomography results: velocity depth slices at 20 m, 40 m, 60 m and 80 m.

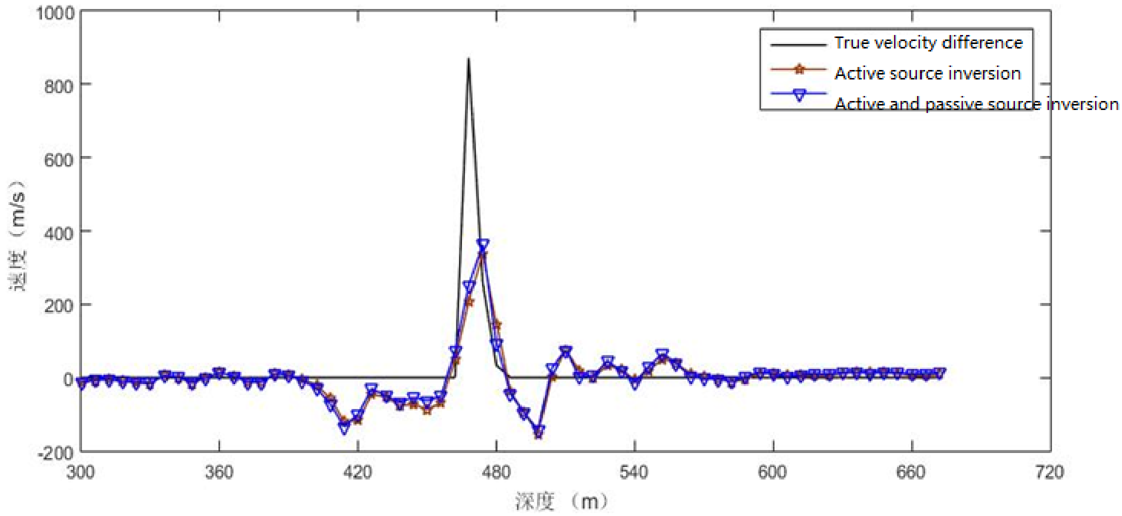

Comparison between the true velocity difference, inversion result with active data only, and inversion result with combining passive and active data (from the middle of the model).

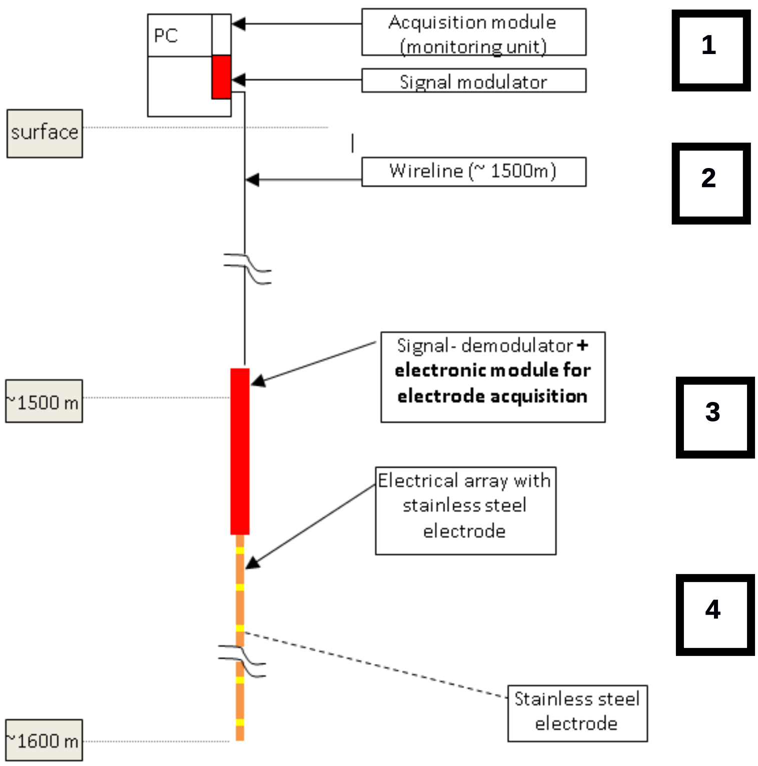

Resistivity device principle

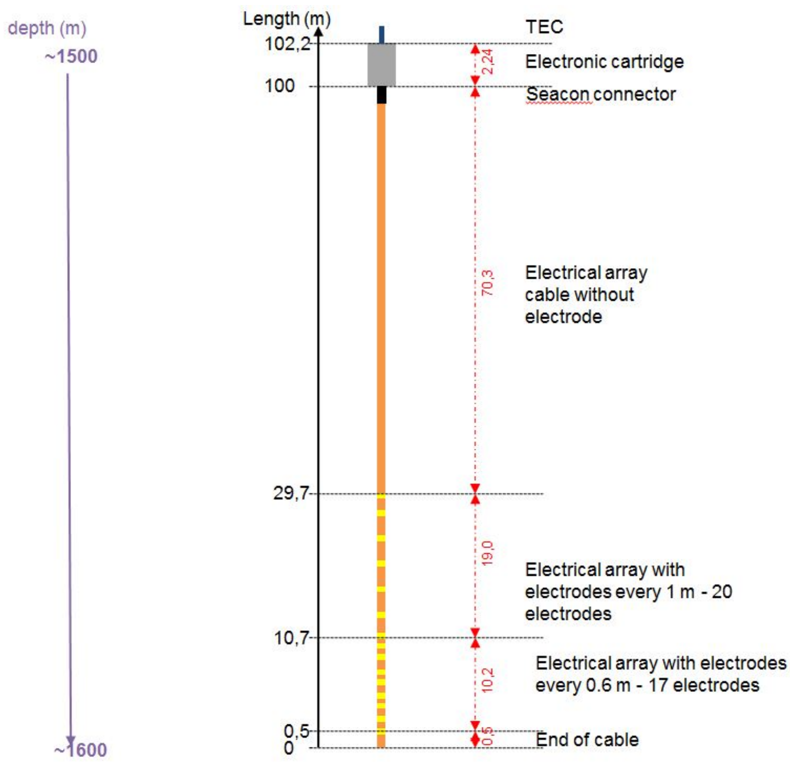

Electrical array design

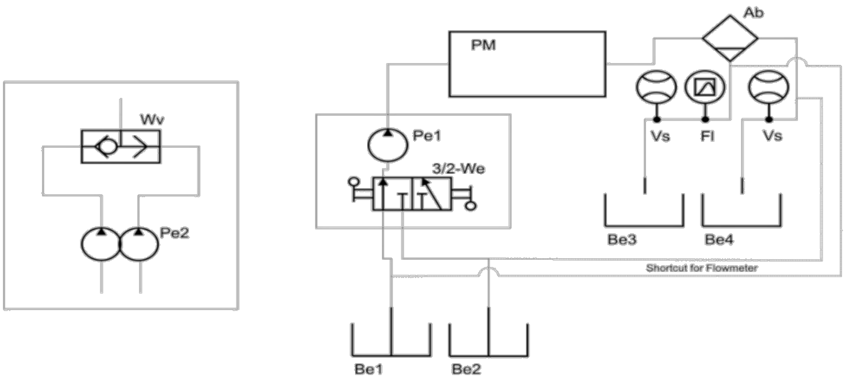

Legend

3/2-We	3/2-way valve	FI	Fluorescence
Ab	Separator	Pe1	Peristaltic pump (1 channel)
Be1	Reservoir (w)	Pe2	Peristaltic pump (2 channel)
Be2	Reservoir (nw)	PM	Porous media
Be3	Waste (w)	Vs	Volumetric flow
Be4	Waste (nw)	Wv	Shuttle valve

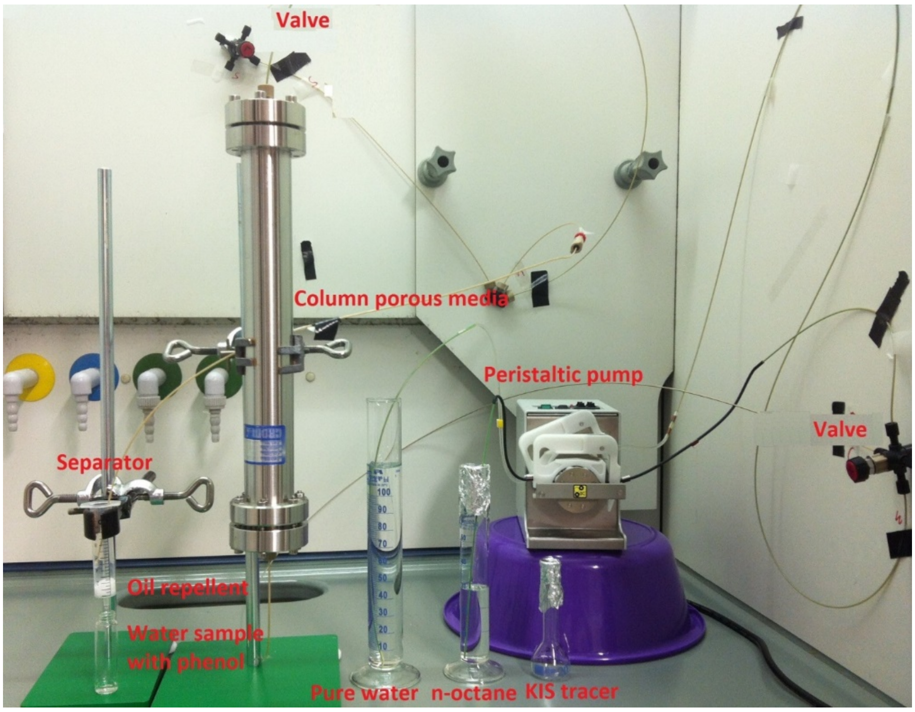

KIS tracers – Laboratory setup

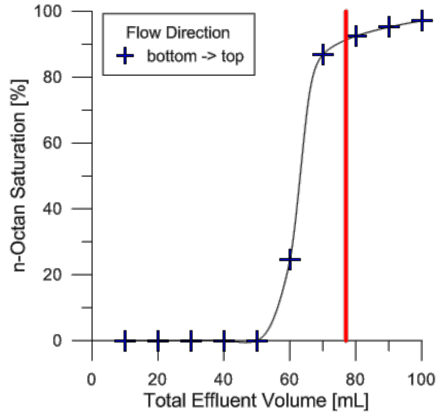

KIS tracers - n-octane breakthrough curve and sample collection from the two-phase flow

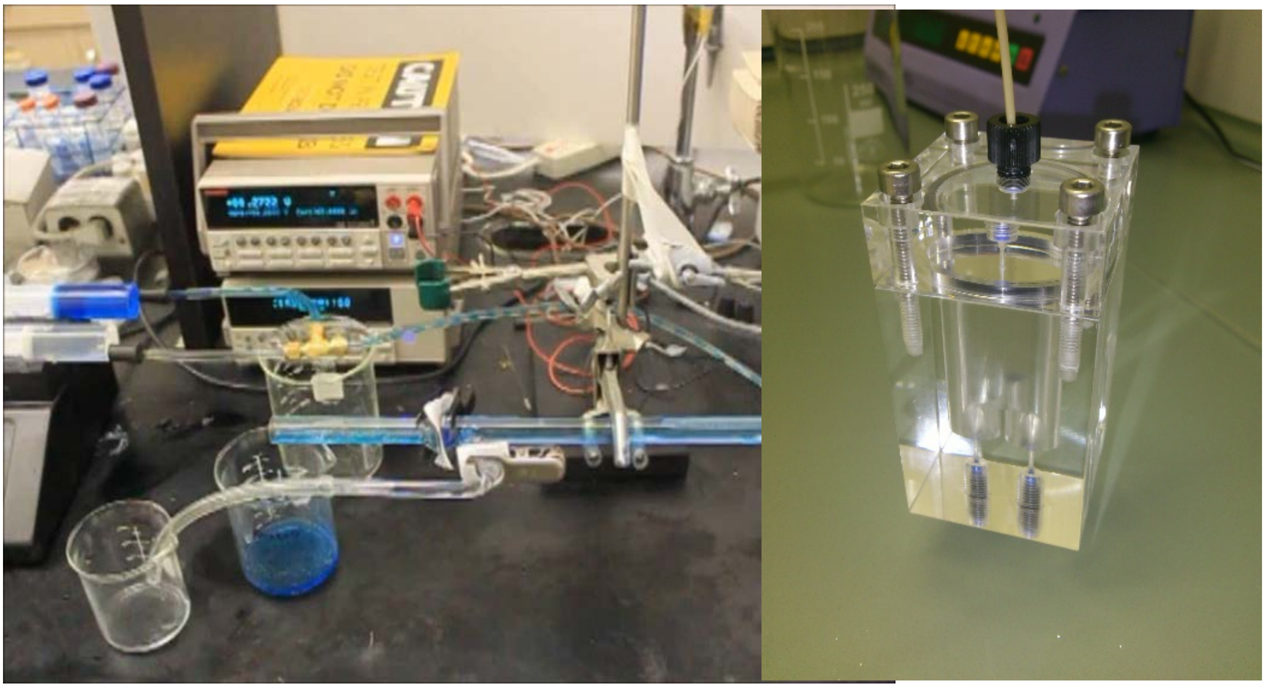

KIS tracers - Non-wetting – wetting phase separator original setup (left) and filter (right) constructed to analyze the KIS tracer, acid and n-octane breakthrough curves.

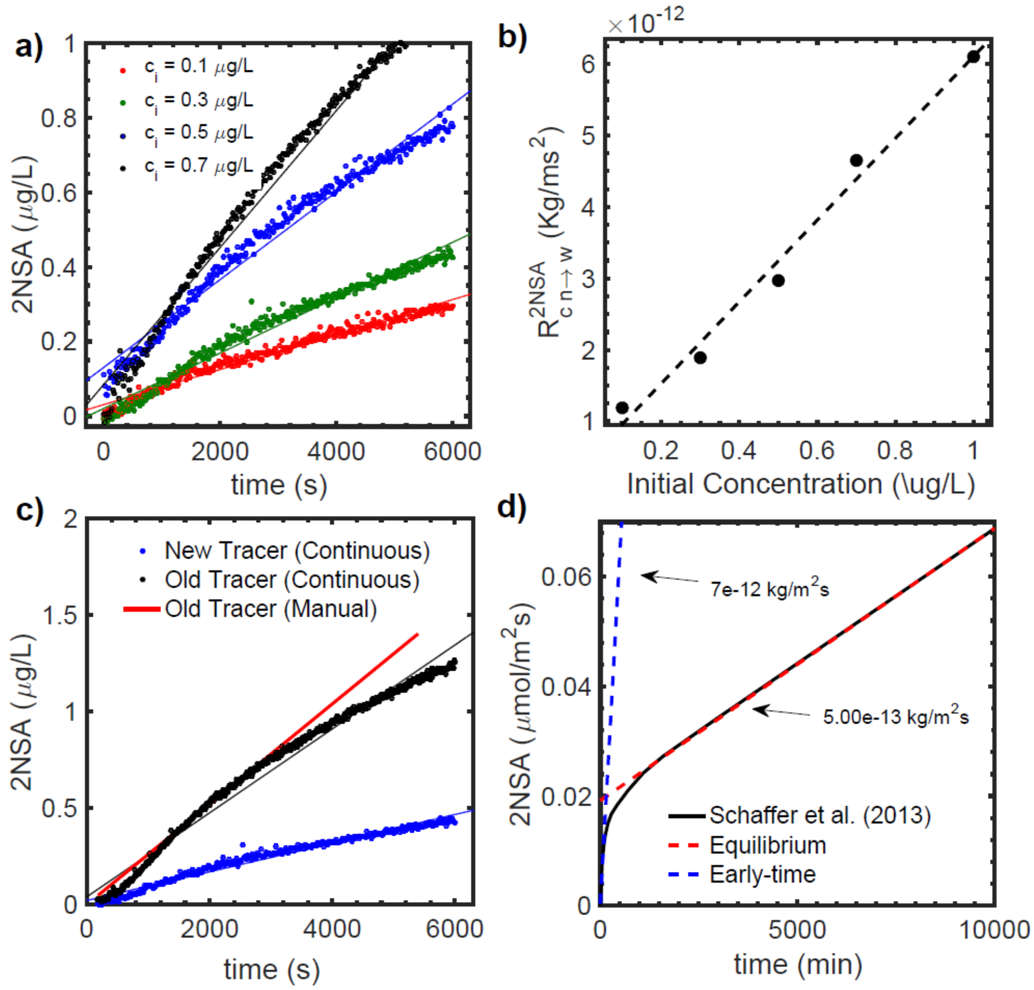

Determination of the hydrolysis kinetic rate using static batch test experiments. a) Continuous measurements of 2NSA over time for different initial concentrations, b) The $R_{c_{n\to w}}^{2NSA}$ for each curve in figure a, c) Shows the 2NSA concentration over time for an initial concentration of 0.5g/L using the new and old tracer and d) is the observed concentration of 2NSA over time taken from Schaffer et al. (2013)

Historic data display of P/T data from downhole gauges.

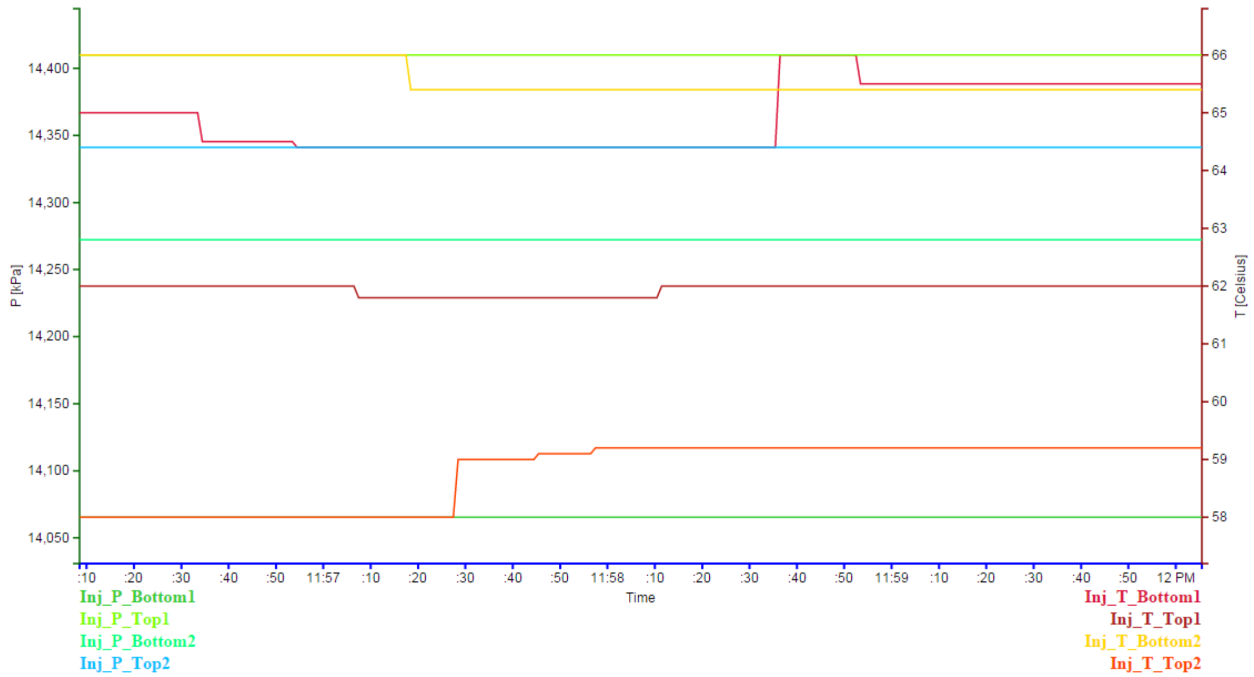

Real time display of P/T data from downhole gauges.

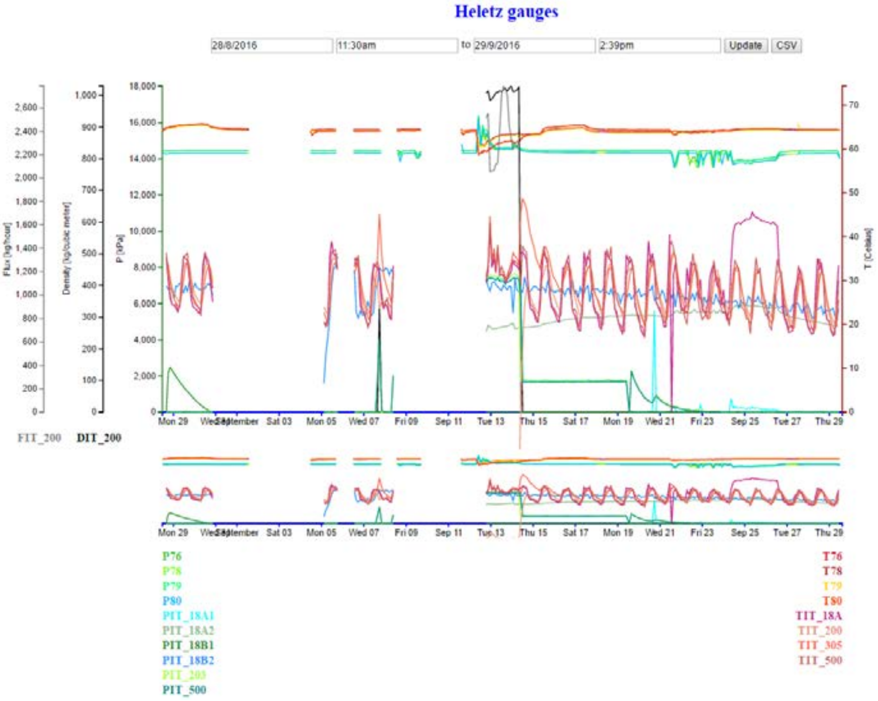

Historic data display of all Heletz gauges.

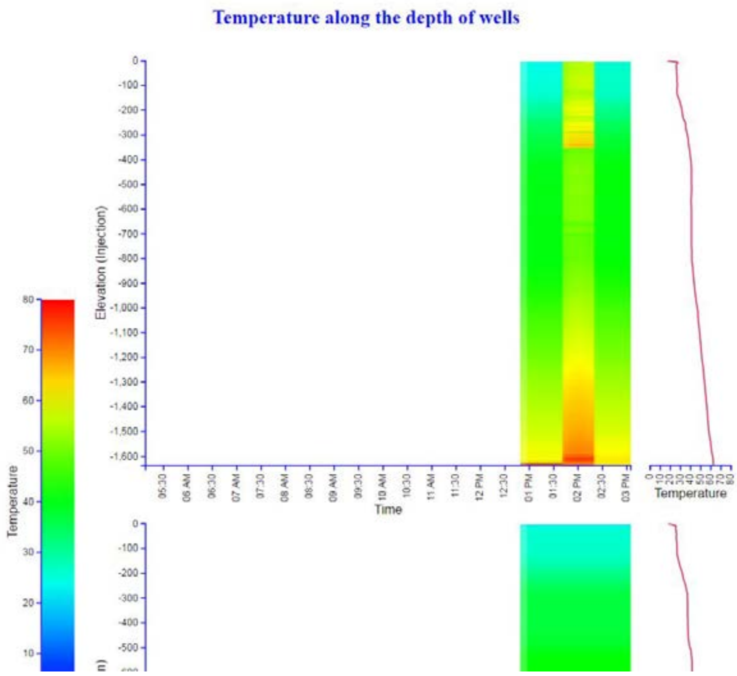

Real-time display of DTS data.

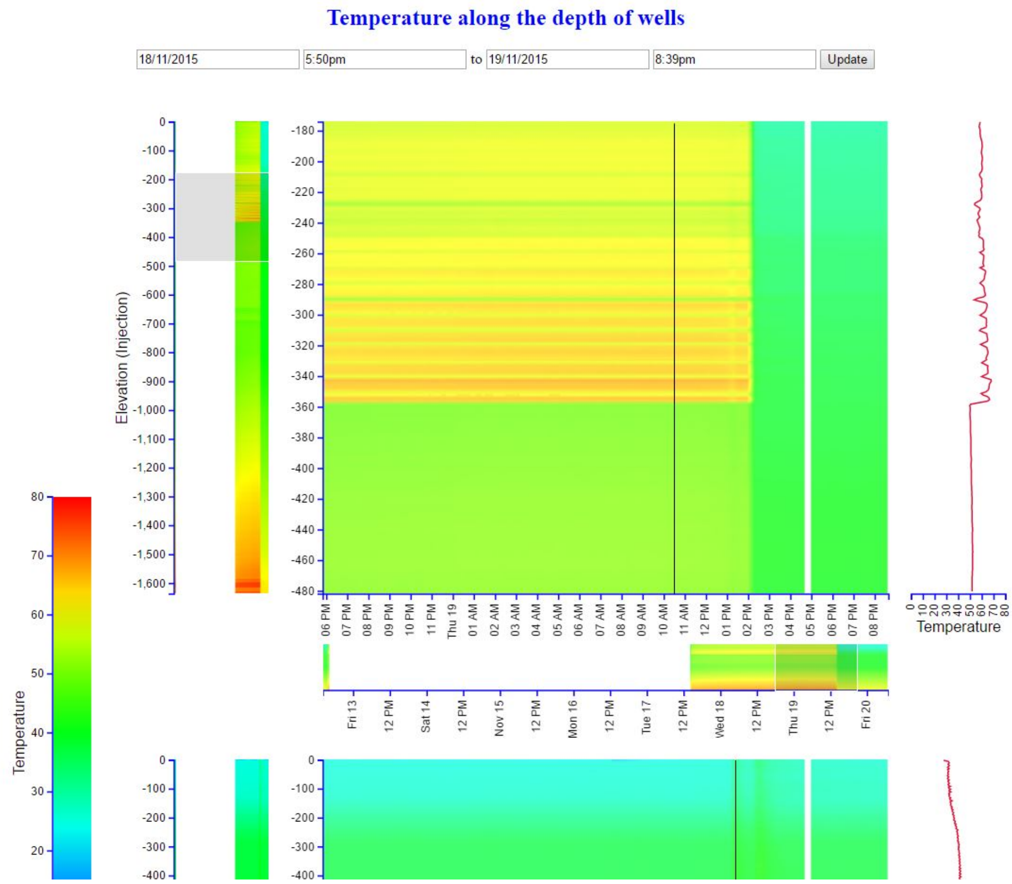

Historic display of DTS data.

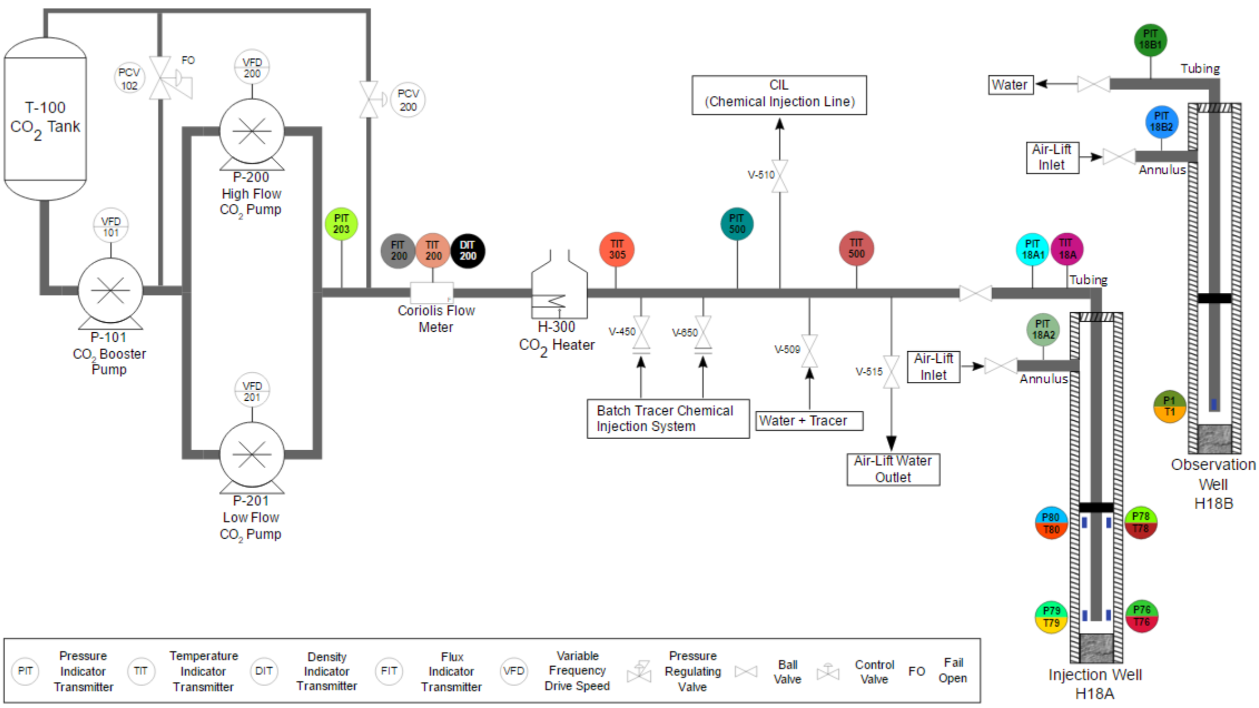

Map of the transmitting sensors connected to the visualization platform.

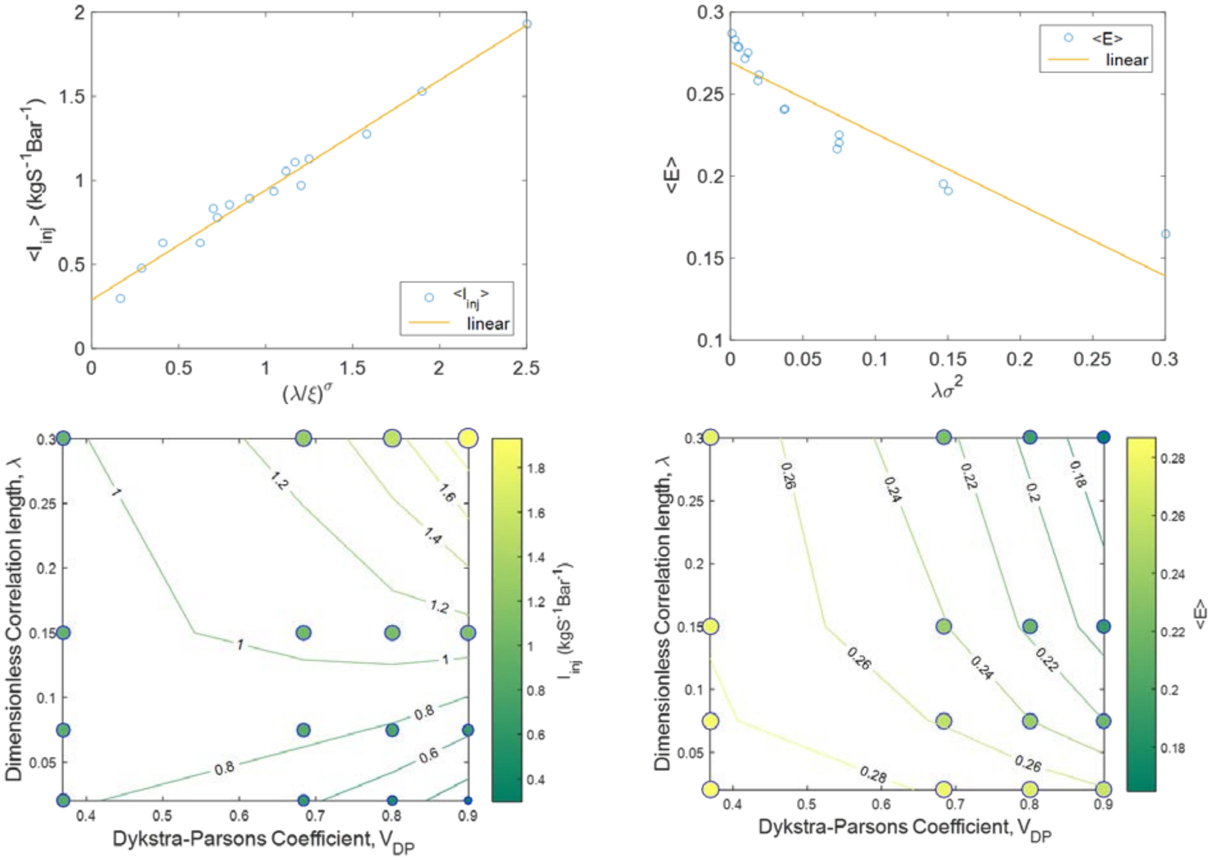

a) Injectivity index and b) storage efficiency as functions of heterogeneity parameter groups, where ξ is a fitting parameter, and c) injectivity index and d) strage efficiency as functions of dimensionless correlation length and Dykstra Parsons coefficient (Tian et al, 2015)

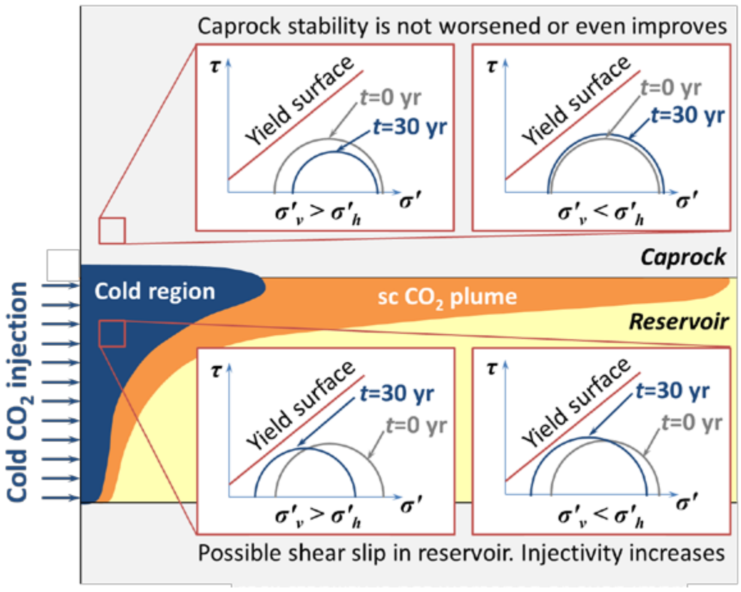

Sum up of the reservoir shear and caprock stability during cold CO_2 injection.

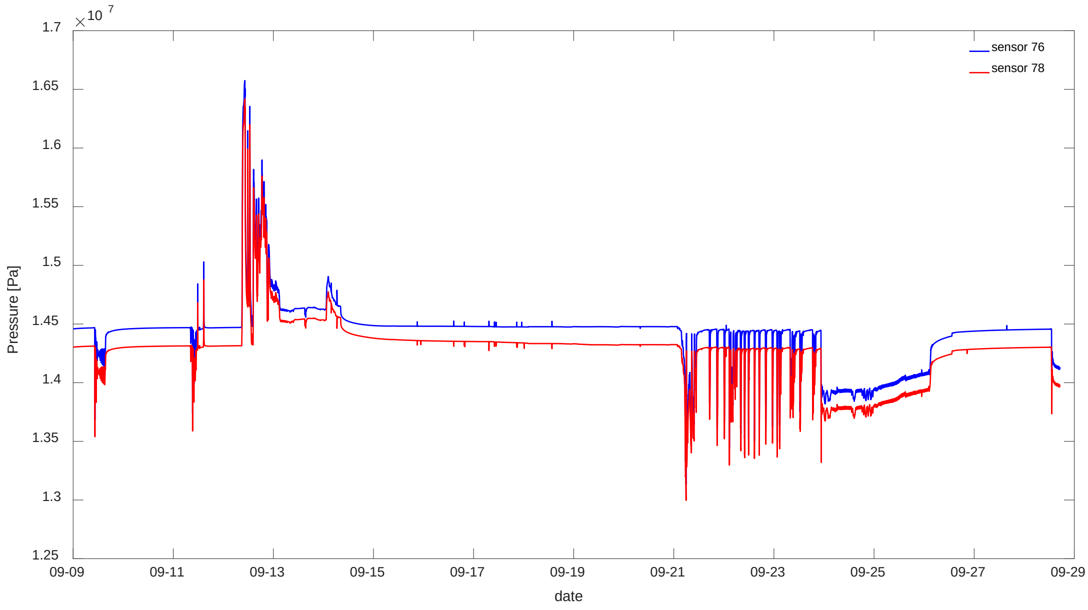

Pressure series for Sensors 76 and 78 in the injection well H18_A.

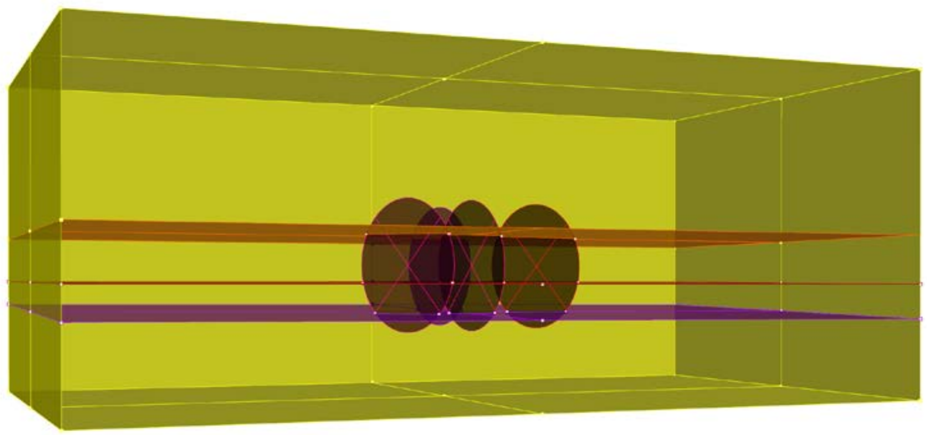

Figure 4.1: Geometry of the pre-existing faults that are assumed to penetrate from the reservoir into the caprock.

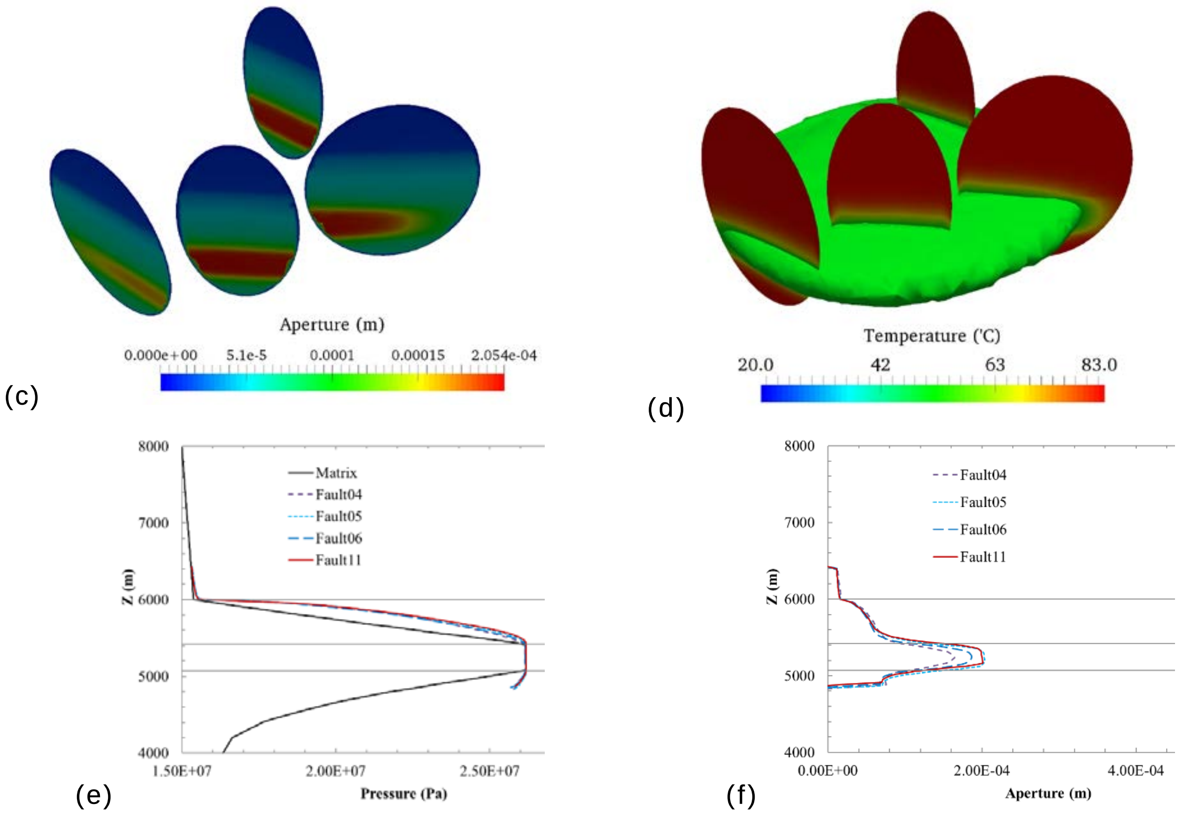

Figure 4.2: The fluid pressure (a), temperature (b), and aperture distribution (c) on the faults, the temperature plume within the reservoir layer (d), pressure profile along a vertical line passing through faults (e), and the aperture profile along a vertical line passing through the centre of the faults (f), after 160 years for the case: E = 10 GPa, T_{inj} = 20°C.

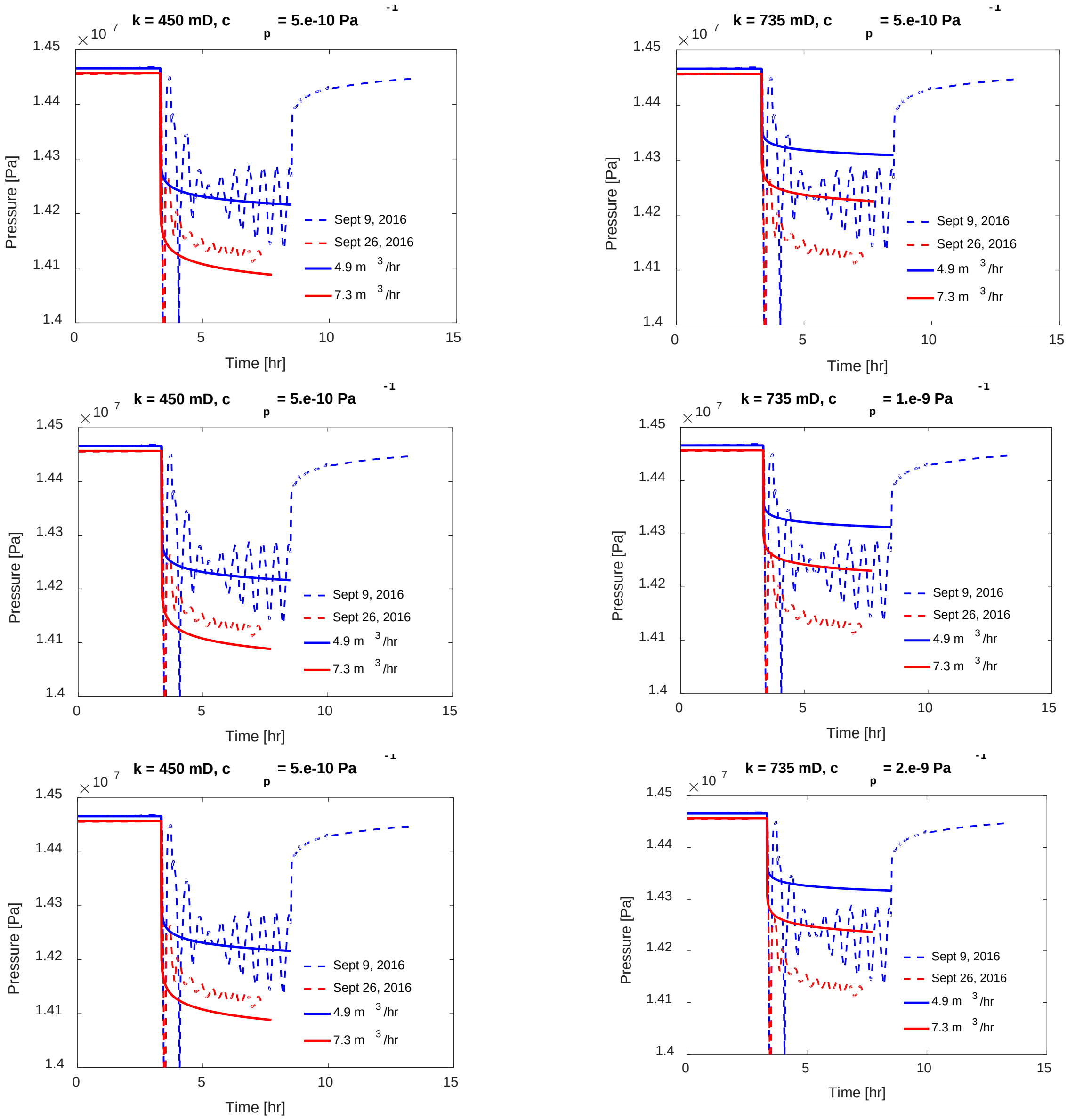

Comparison between hydraulic test data (see dash lines; both on September 9th and 26th) and the Theis solution (solid lines) for different parameter values of permeability and pore compressibility. Note that in each subplot, the same permeability is used for both tests, regardless of whether there is CO_2. The flow rates for both dates are averaged from pump readings.

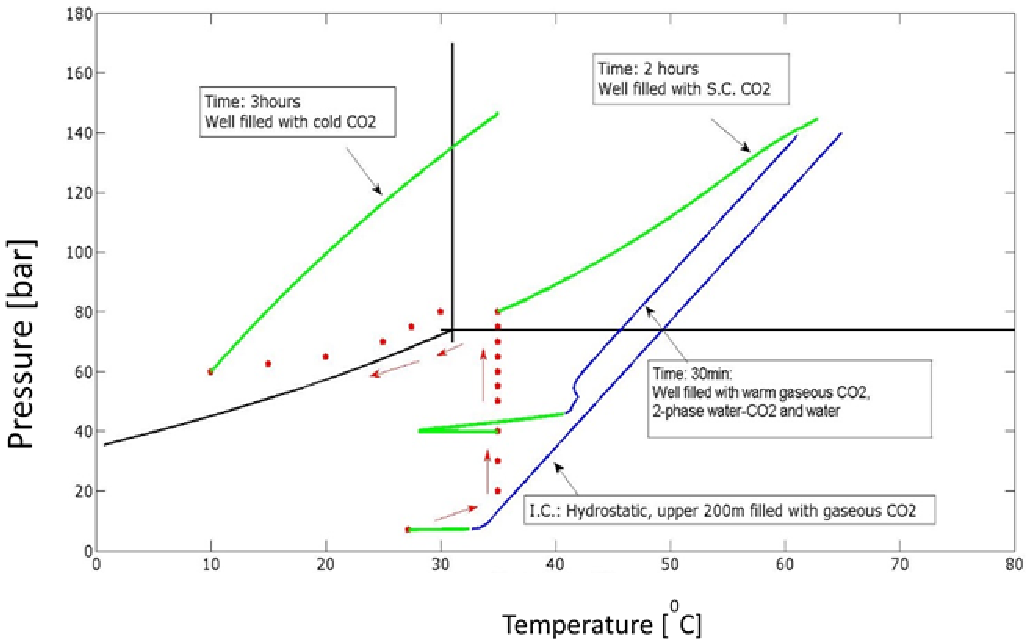

Injection sequence for “cold injection” in the phase space.

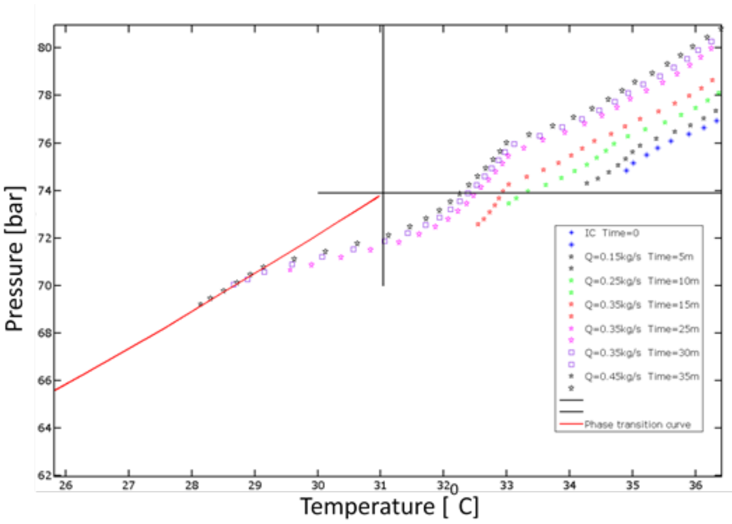

Well flow – CO_2 release sequence in the phase space.

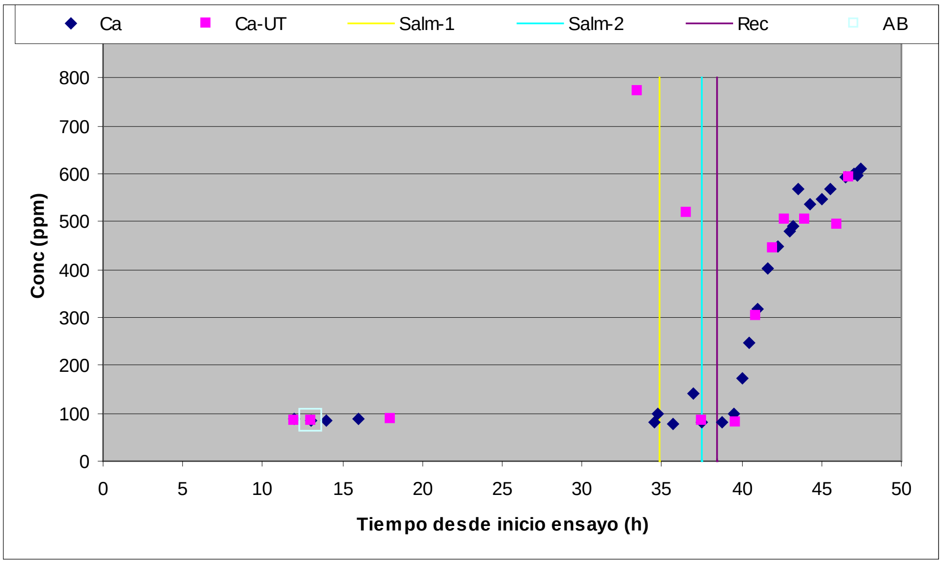

Calcium concentration in the injected brines from t=0 to t= 38h and in the pumping fluid for t > 38h during the push-pull field test in Hontomin.

	dissolved CO_2 [mass/mass %]	CO_2 injection rate [ton/year]
CO_2 at 30°C	7.80	1,000,000
CO_2 at 67°C	8.04	1,000,000

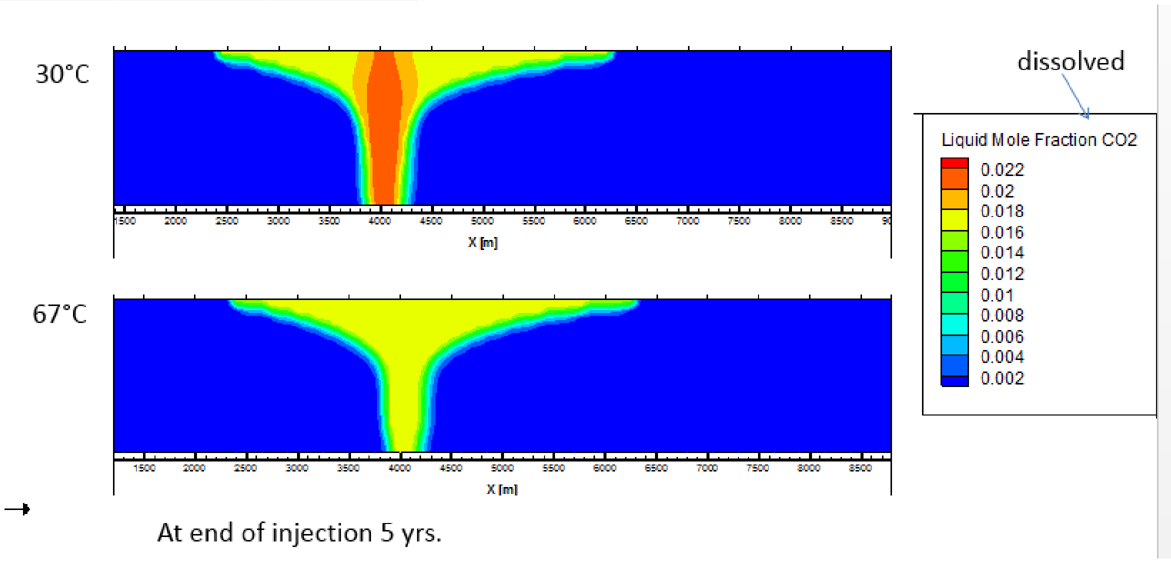

Liquid mole fraction of CO_2 moles in water to total number of moles of water + fraction dissolved CO_2.

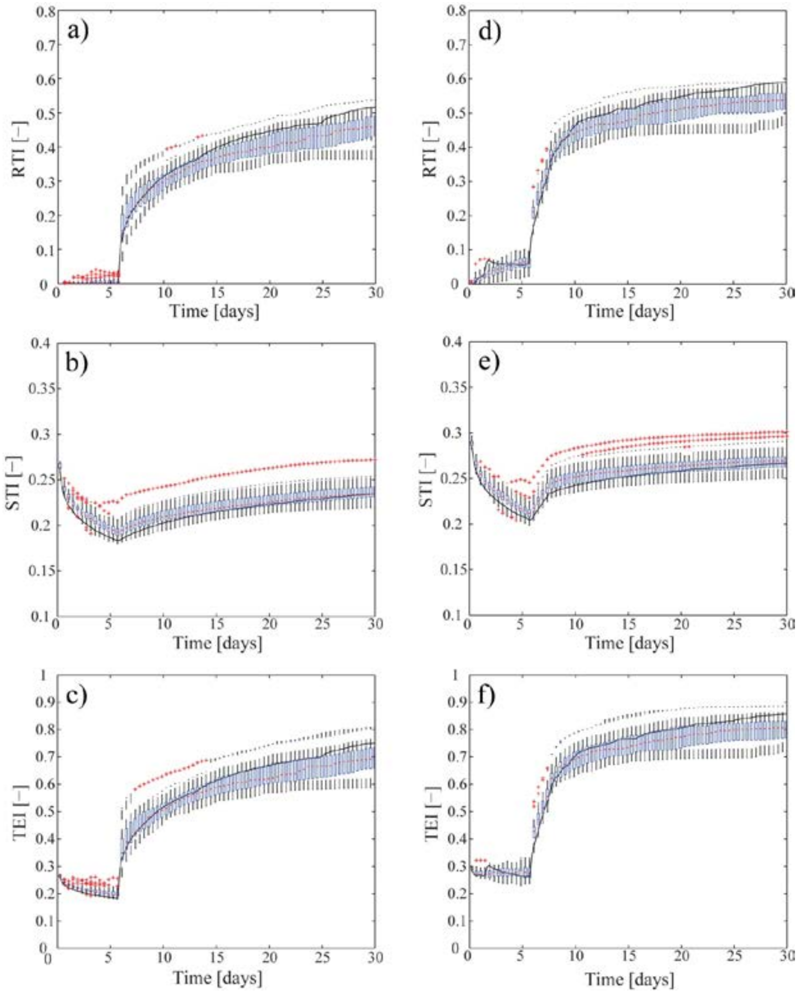

Comparison of the RTI, STI and TEI for the case of formations with a homogeneous and heterogeneous k/φ-field when employing (a-c) a 'conventional injection' strategy or (d-f) a 'mixed co-injection and chased injection' strategy. The black line represents the result of the homogeneous case. The results of the heterogeneous cases are illustrated by boxplots. The red line indicates the median, the edges of the box represent the 25th and 75th percentiles and the whiskers indicate the extreme values (outliers not included).

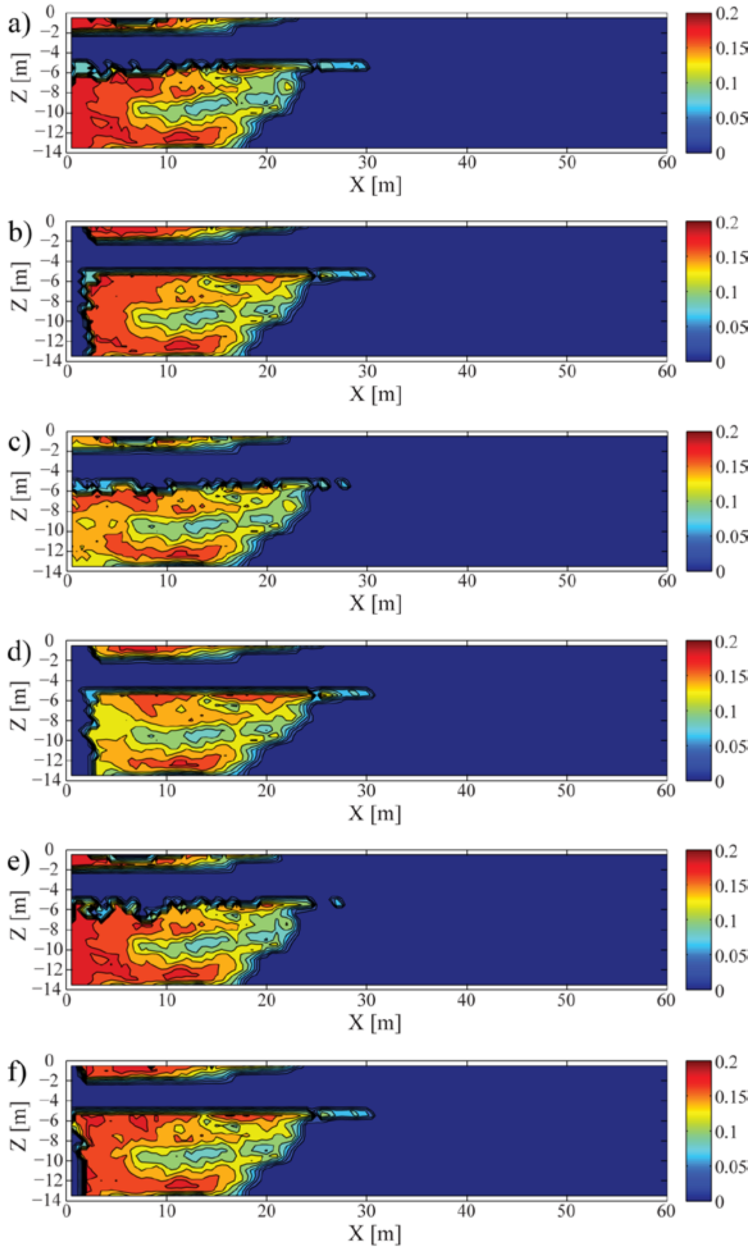

The residual gas phase saturation (S_{gr}) in a heterogeneous formation (exhibiting high trapping) at day 30 from the start of injection for the injection strategies; (a) 'conventional injection', (b) 'chased injection', (c) 'co-injection', (d) 'mixed co-injection and chased injection', (e) 'cyclic injection' and (f) 'small WAG injection'.

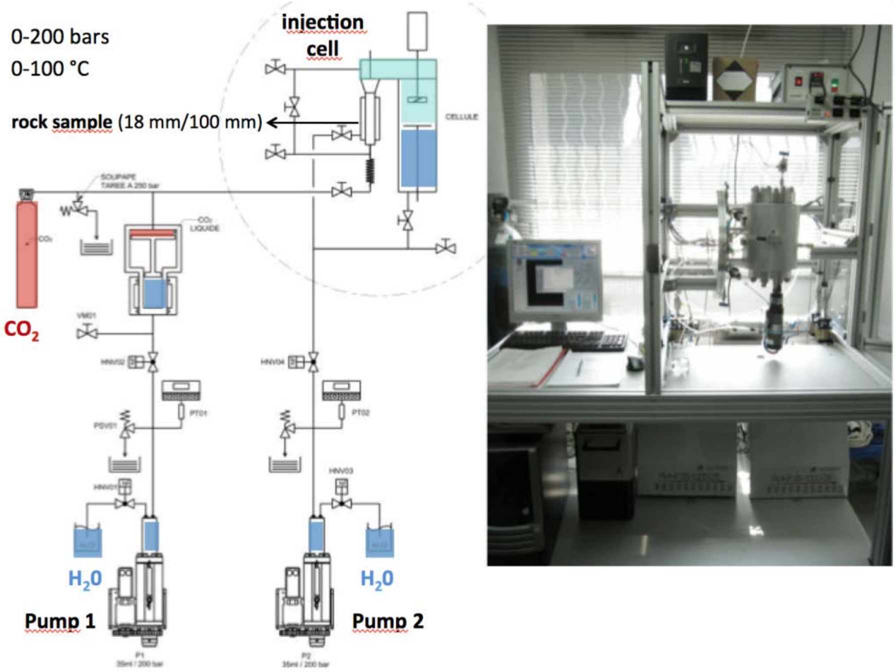

Diagram (left) and photograph (right) of the experimental bench ICARE 5 for carbonation experiments (reactive mineral slurry)

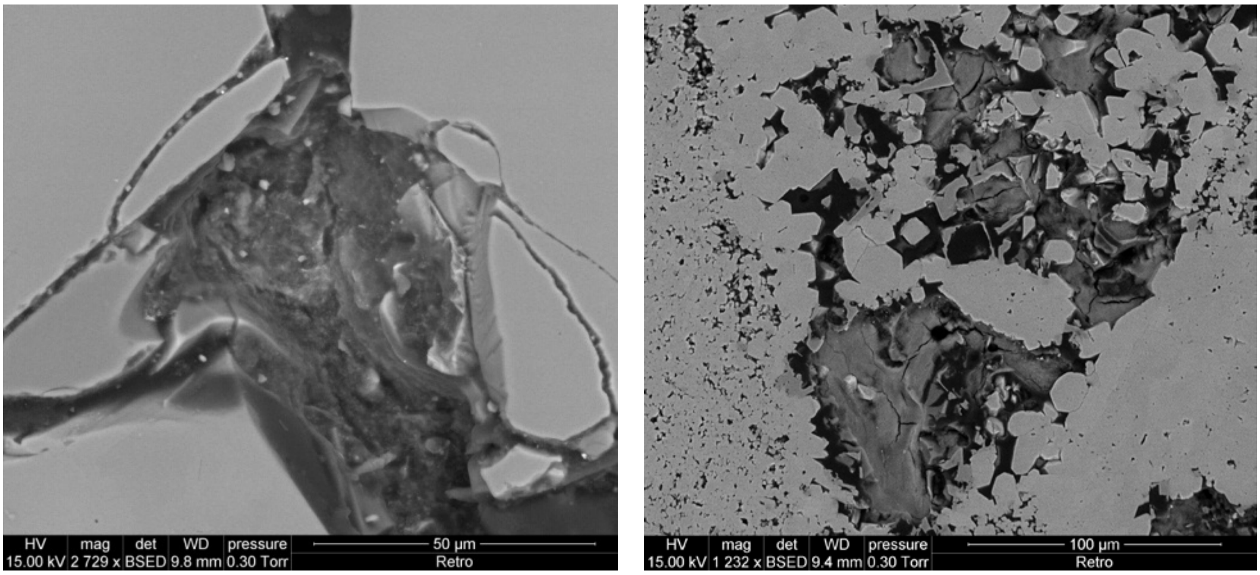

Solidified silica gel in Fontainebleau sandstone (left) and limestone (right).

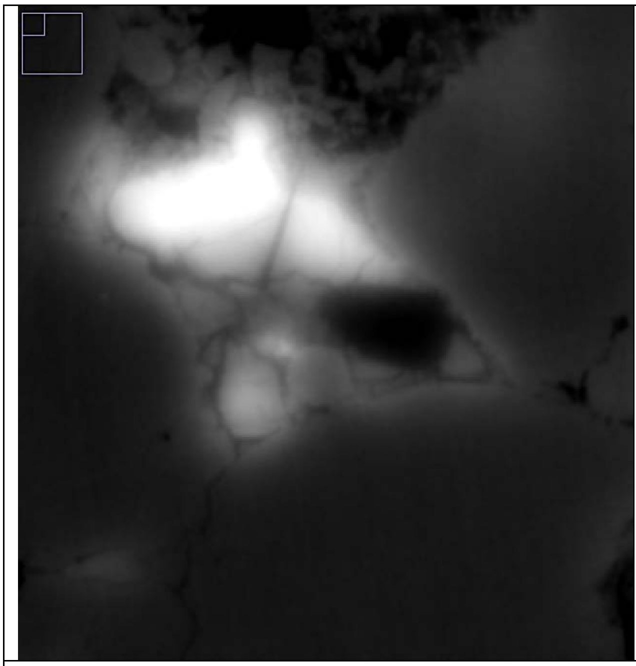

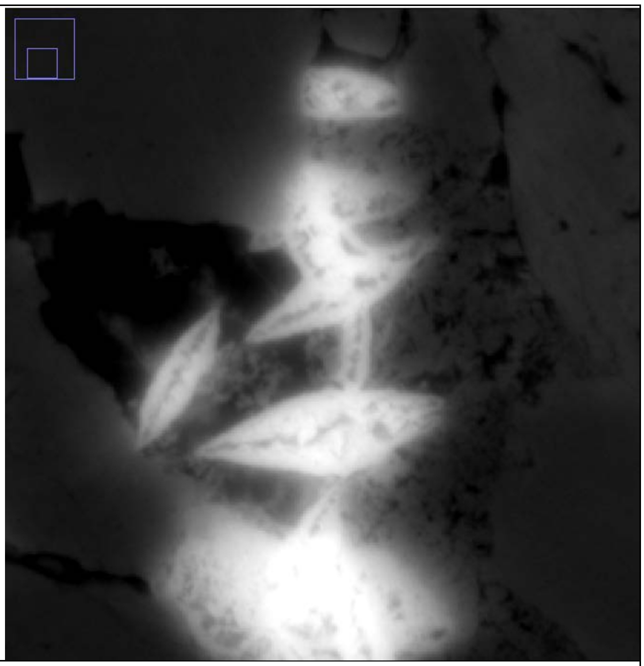

Cross-section of 3D X-ray micro-tomogaphy image of Berea sandstone with partial filling of the pore space by the solgel (white color) that was doped with an X-ray absorbent component (tantalum).

Figure 6.2: Shrinking observed when gel solidification takes place.

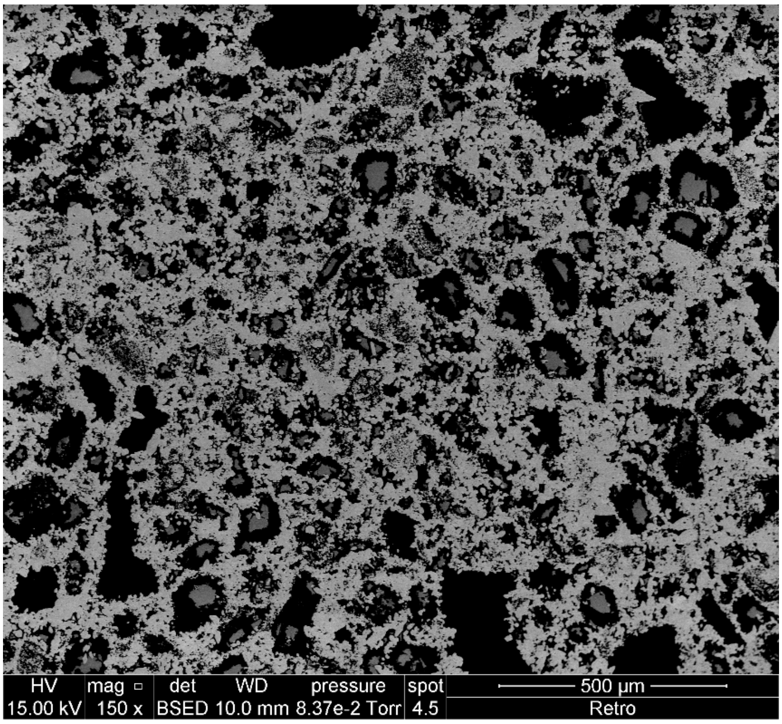

Figure 6.5: SEM image showing solgel filling the porous of the carbonate sample.

General overview of TRUST website.

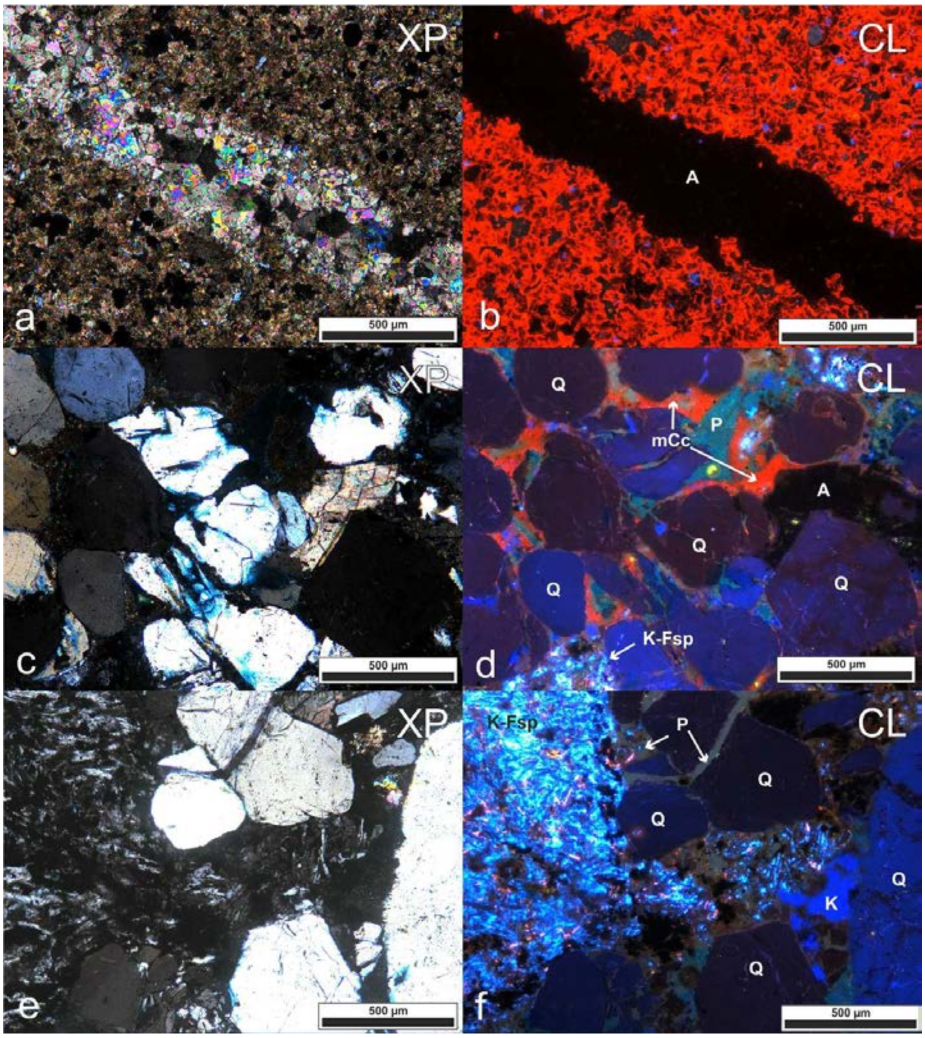

Representative photomicrographs of investigated rock samples in both crossed polarized light (XP) and cathodoluminescence imaging (CL). **a / b**: limestone (caprock) with calcite matrix (red) and detrital quartz (non-luminescent) and K-feldspar grains (blue); **c / d:** fine grained sandstone (f1) with micritic calcite cement (red to orange) and a single euhedral ankerite crystal (non-luminescent); **e / f**: coarse grained sandstone (g1) with kaolinite cement (dark blue) and illite cement (dark brown rims), calcite cement is missing. The grain to the left mostly consisting of bright blue luminescing potassium-feldspar is a volcanic lithoclast, the syenitic-trachytic texture is best noticeable in the XP image. A=sparitic Ankerite (cement), Q=detrital quartz grain, K-Fsp=potassium-feldspar, mCc=micritic Calcite cement, P=pore space.

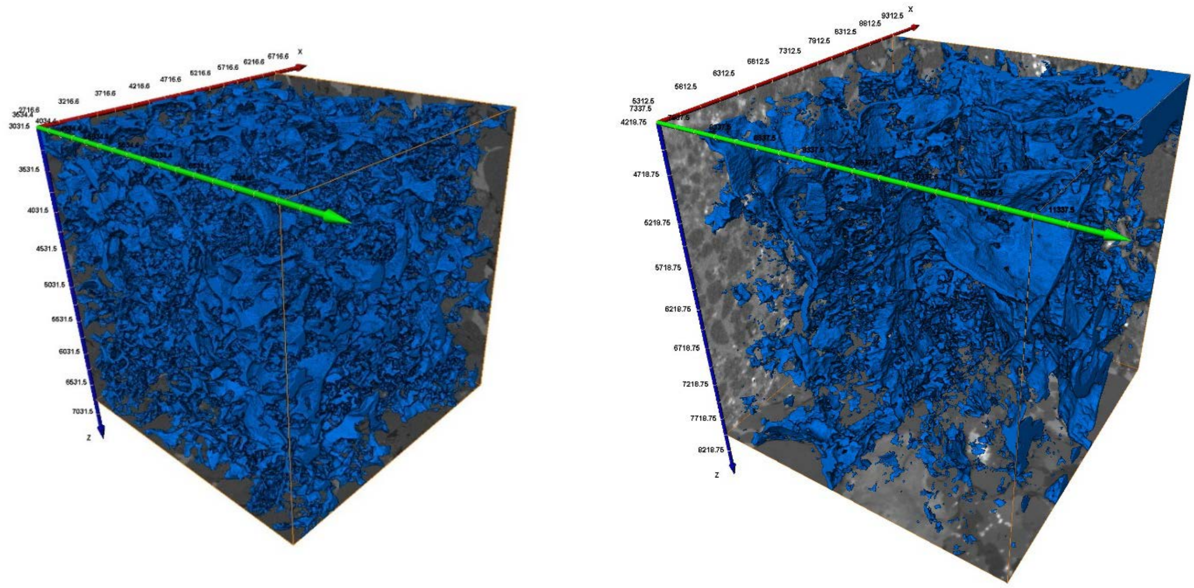

Visualization of the different types of pore connectivities for the fine grained (left hand side) and coarse grained (right hand side) Heletz sandstone that have been used as for permeability tensor modeling based on μCT scans.